

JPET # 265330

Simultaneous Target-Mediated Drug Disposition (TMDD) Model for Two Small-Molecule Compounds Competing for Their Pharmacological Target: Soluble Epoxide Hydrolase

Nan Wu¹, Bruce D. Hammock², Kin Sing Stephen Lee^{3,4*}, Guohua An^{1,*}

¹ Division of Pharmaceutics and Translational Therapeutics, College of Pharmacy, University of Iowa, Iowa city, Iowa

² Department of Entomology and Nematology and UCD Cancer Research Center, University of California at Davis, Davis, California

³ Department of Pharmacology and Toxicology, Michigan State University, East Lansing, Michigan

⁴ Department of Chemistry, Michigan State University, East Lansing, Michigan

JPET # 265330

Running title: TMDD Model for Two Potent Small-Molecule sEH Inhibitors

***Correspondence:**

Guohua An, MD, Ph.D.

Division of Pharmaceutics and Translational Therapeutics,
College of Pharmacy, University of Iowa,
115 S Grand Ave, Iowa City, IA, 52242, USA.
E-mail: guohua-an@uiowa.edu

Kin Sing Stephen Lee, Ph.D.

Department of Pharmacology and Toxicology
Department of Chemistry,
Michigan State University,
1355 Bogue St, East Lansing, MI-48823
[Email: sing@msu.edu](mailto:sing@msu.edu)

Number of text pages: 31

Number of tables: 3

Number of figures: 11

Number of references: 30

Number of words

Abstract: 248

Introduction: 739

Discussion: 1,085

Keywords: target-mediated drug disposition; mathematical modeling and simulation; TMDD model, Soluble Epoxide Hydrolase inhibitors; target occupancy

JPET # 265330

ABSTRACT

1-(1-propanoylpiperidin-4-yl)-3-[4-(trifluoromethoxy)phenyl]urea (TPPU) and 1-(4-trifluoromethoxy-phenyl)-3-(1-cyclopropanecarbonyl-piperidin-4-yl)-urea (TCPU) are potent inhibitors of soluble epoxide hydrolase (sEH) which have much better efficacy in relieving nociceptive response than the FDA-approved drug, gabapentin, in a rodent model of diabetic neuropathy. Experiments conducted in sEH-knock-out mice or with coadministration of a potent sEH displacer demonstrated that the pharmacokinetics of TPPU and TCPU were influenced by the specific binding to their pharmacologic target sEH, a phenomenon known as target-mediated drug disposition phenomenon (TMDD). To quantitatively characterize the complex pharmacokinetics of TPPU and TCPU and gain better understanding on their target occupancy, population pharmacokinetics analysis using a nonlinear mixed-effect modeling approach was performed in the current study. The final model was a novel simultaneous TMDD interaction model, where TPPU and TCPU compete for sEH, with TCPU binding to an additional unknown target pool with larger capacity which we refer to a refractory pool. The total amount of sEH enzyme (R_{max1}) in mice was predicted to be 16.2 nmol, which is consistent with the experimental value of 10 nmol. The dissociate rate constants (k_{off}) of TPPU and TCPU were predicted to be 2.24 h^{-1} and 2.67 h^{-1} , respectively, which is close to the values obtained from in vitro experiments. Our simulation result predicted that, 90% of the sEH will be occupied shortly after a low dose of 0.3 mg/kg TPPU administration, with $\geq 40\%$ of sEH remaining to be bound with TPPU for at least 7 days. Further efficacy experiments are warranted to confirm the predicted target occupancy.

JPET # 265330

SIGNIFICANCE STATEMENT:

Although TMDD models have been well documented, most of them were established in a single compound scenario. Our novel model represents the first TMDD interaction model for two small-molecule compounds competing for the same pharmacological target.

JPET # 265330

1. INTRODUCTION

Soluble epoxide hydrolase (sEH) is a major enzyme involved in metabolizing epoxy-polyunsaturated fatty acids such as epoxyeicosatrienoic acids (EETs) into much less active dihydroxyeicosatrienoic acids (DHETs)(Tu et al., 2018), leading to partial or complete loss of their initial biological activities. sEH is highly expressed in the liver, kidney, heart, lung, intestine, brain, and vasculature of mammals, and its increased expression is associated with inflammation and several diseases (Enayetallah et al., 2004; Sura et al., 2008; Marowsky et al., 2009). sEH is also presented in red blood cell in small amount (Lee et al., 2019). Because inhibition of sEH stabilizes endogenous EETs, sEH represents a promising therapeutic target for the treatment of inflammation, pain, cardiovascular diseases, and a variety of other disease usually involving mitochondrial dysfunction and endoplasmic reticulum stress (Lee et al., 2013; Lee et al., 2014; Wagner et al., 2017; Tu et al., 2018).

Effort has been made toward the discovery of the sEH inhibitors in the past decades. Among the various sEH inhibitors identified, 1-(1-propanoylpiperidin-4-yl)-3-[4-(trifluoromethoxy)phenyl]urea (TPPU) and 1-(4-trifluoro-methoxy-phenyl)-3-(1-cyclopropanecarbonyl-piperidin-4-yl)-urea (TCPU) represent two particularly promising candidates due to their potent inhibition on sEH (Ostermann et al., 2015; Goswami et al., 2016; Yao et al., 2016; Guo et al., 2018). Both TPPU and TCPU have demonstrated much better efficacy in relieving nociceptive response than the FDA-approved drug, gabapentin, in a rodent model of diabetic neuropathy (Lee et al., 2019). *In vitro* binding kinetics experiments showed that TPPU and TCPU have small dissociation rate constants ($k_{off}=(8.52\pm 0.47)\times 10^{-4}\text{ s}^{-1}$ and $(9.9\pm 0.1)\times 10^{-4}\text{ s}^{-1}$ respectively), which indicates their tight binding with sEH (Liu et al., 2012; Lee et al., 2014). In addition, both TPPU and TCPU have high affinity to sEH ($k_d=2.5\text{ nM}$ and 0.9 nM , respectively).

JPET # 265330

Interesting characteristics in the pharmacokinetic profiles of TPPU and TCPU were observed in our novel displacement experiment conducted recently in both wild-type mice and sEH-global knockout mice (Lee et al., 2019). We have the following key observations: 1) TPPU plasma concentration decreased rapidly in sEH-knockout mice and cannot be measured after 48 hrs using a highly sensitive mass spectrometry method with the limit of detection ≤ 0.4 nM. In contrast, TPPU pharmacokinetics in wild-type mice has a much longer terminal phase, with TPPU plasma concentrations being measurable past 312 hours. This phenomenon may be explained by the tight binding of TPPU with sEH, and the corresponding slow dissociation process of TPPU from the TPPU-sEH complex in tissues. 2) When the wild-type mice dosed with TPPU at time 0 followed by a dose of TCPU at 168 hrs (i.e. 1 week later), the TPPU plasma profile showed two peaks, with the first TPPU peak (~ 2 hrs) observed shortly after TPPU dose and the second TPPU peak (~170 hrs) observed shortly after the TCPU dose. The second peak was not observed in sEH-knockout mice following the same dosing regimen. 3) Interestingly, we observed TCPU plasma concentration peaks right after time 0 (TPPU added) in one group of re-used mice that was administrated TCPU 2 weeks previously, which accidentally supported the hypothesis that TCPU could also be displaced by TPPU reversely. Our findings strongly suggested that the pharmacokinetics of TPPU and TCPU were influenced by the specific binding to their pharmacologic target sEH, a phenomenon known as target-mediated drug disposition phenomenon (TMDD) (Levy, 1994; An, 2020).

It is known that compounds exhibiting TMDD usually have complex and nonlinear pharmacokinetics, and the dose regimen selection can be quite challenging since the relationship among dose, drug exposure, and response is no longer intuitive. To optimize the dose regimen, it is important to utilize pharmacometric modeling approaches to elucidate the quantitative

JPET # 265330

relationship between drug exposure and response. The goal of the current study was to develop a TMDD mathematical model to quantitatively characterize the complex pharmacokinetics of TPPU and TCPU we observed in mice and gain better understanding on their target occupancy. The first TMDD mathematical model was proposed by Mager and Jusko in 2001 (Mager and Jusko, 2001). Several different TMDD models have been published since then (Grimm, 2009; Ait-Oudhia et al., 2010; Gibiansky and Gibiansky, 2010; Yan et al., 2012; Dua et al., 2015). However, most reported TMDD models were developed in a single compound scenario, and therefore cannot be adapted directly to characterize the TPPU and TCPU data we have. In the current study we present a novel simultaneous TMDD interaction model, where TPPU and TCPU compete for their pharmacologic target sEH with TCPU unexpectedly binding to an additional unknown target pool with larger capacity which we refer to a refractory to degradation pool.

JPET # 265330

2. MATERIALS AND METHODS

2.1 Data Source

TPPU and TCPU pharmacokinetics displacement data in mice came from a published study and were used for development of the TMDD pharmacokinetics model (Lee et al., 2019). The chemical structures of TPPU and TCPU are shown in **Supplemental Table 1** and study design is shown in **Figure 1**. As shown in **Figure 1**, two experiments were conducted, with 4 treatment groups in experiment 1 and 3 treatment groups in experiment 2 (4-6 mice/group). In experiment 1, wild-type mice received a 0.3 mg/kg dose of TPPU subcutaneously (S.C.) at time 0 on the 1st day followed by either blank vehicle (Group 1) or 3 mg/kg TCPU (Group 2) at 168 hours on the 7th day. Similarly, sEH knockout mice in experiment 1 received S.C. 0.3 mg/kg dose of TPPU at time 0 on the 1st day followed by either blank vehicle (Group 3) or 3 mg/kg TCPU (Group 4) at 168 hours on the 7th day. In experiment 1, blood samples were collected at 0, 0.25, 0.5, 1, 2, 4, 6, 8, 24, 48, 72, 96, 120, 144, 168, 168.25, 168.5, 168, 169, 170, 172, 174, 176, 192, 216, 264, 312 hours. In experiment 2, wild-type mice received a S.C. 0.3 mg/kg dose of TPPU at time 0 on the 1st day followed by TCPU 1 mg/kg (Group 1), 10 mg/kg (Group 2) or 0.3 mg/kg (Group 3) at 168 hours on the 7th day. The wild-type mice used in Group 3 of experiment 2 were reused from a previous experiment, where the mice were given a weak sEH inhibitor, mTPPU (**Supplemental Figure 1**), at 1 mg/kg s.c 3 weeks ago followed by 3mg/kg TCPU s.c. one weeks from the administration of mTPPU. Blood samples from experiment 2 were collected through tail nick at similar time points as that in experiment 1. The concentrations of TPPU and TCPU in mice plasma were quantified using a well characterized and quantitative LC/MS/MS assay as published previously (Lee et al., 2019). Lower limit of quantification (LLOQ) for both TPPU and TCPU was 0.49 nM. The inter-

JPET # 265330

day and intra-day accuracy and precision of TPPU and TCPU were all within 15%. Detailed bioanalytical assay information has been reported previously (Lee et al., 2019).

2.2 Population Pharmacokinetics modeling

All pharmacokinetics data for TPPU and TCPU from both *in vivo* displacement experiments were analyzed simultaneously using the nonlinear mixed effect modeling approach with NONMEM (Version 7.4.3; Icon Development Solutions, Ellicott City, Maryland) interfaced with Pirana (version 2.9.9, <http://www.pirana-software.com/>). The first-order conditional estimation method with interaction (FOCEI) and a user-defined subroutine (ADVAN13) were used to estimate the population mean values of the pharmacokinetics parameters, inter-individual variability (IIV) and residual variability (RV) between observed and individually predicted plasma TPPU and TCPU concentrations. Sigmaplot and RStudio (version 1.0.143, <https://www.rstudio.com/>) were used for graphical analysis and data handling. Data from the reused mice (experiment 2 3rd group) were excluded to avoid the potential inference from the previous experiment even though this group accidentally revealed the TMDD characteristics of TCPU. TCPU data in knock-out mice was also excluded due to small sample size with outlier data. BLQ data were also excluded.

2.2.1 Structural model evaluated

TPPU data from sEH knockout mice were used to build the TPPU base structure model. Among the different models tested (e.g. 1- or 2-compartment models), the one compartment model with first-order absorption and linear elimination was found to best characterize TPPU disposition in sEH knock-out mice. This base structure was then incorporated with the TMDD component(s) to characterize TPPU pharmacokinetics from the wild-type mice. During model building process,

JPET # 265330

various TMDD model structures for TPPU and TCPU have been evaluated. Followings are several representative models (Model structure is shown in **supplemental Figure 2**):

Model with one TMDD component (supplemental Figure 2a):

In this model, both TPPU and TCPU have same central pharmacophore in the model (i.e. one-compartment, 1st order absorption and elimination), but only TPPU has a TMDD component, TPPU interacted with sEH with a second-order association rate constant (k_{on}) to form a TPPU-sEH complex. TPPU-sEH complex dissociated back to free sEH target and free drug with the first-order dissociation rate constants k_{off} . The compacity of sEH target (R_{max1}) remained constant. The TCPU plasma concentration was assumed to directly affect the k_{off} of TPPU.

Model with two TMDD components (supplemental Figure 2b):

In this model, in addition to their base structure, both TPPU and TCPU have TMDD components. TPPU and TCPU can interact with sEH with a second-order association rate constant ($k_{on,TPPU}$ and $k_{on,TCPU}$, respectively) to form a drug-sEH complexes. TPPU-sEH and TCPU-sEH can dissociate back to free drug and free sEH target with the first-order dissociation rate constants ($k_{off,TPPU}$ and $k_{off,TCPU}$, respectively).

Model with two TMDD components plus MM process (supplemental Figure 2c):

This model was built on top of the model with two TMDD components, with an additional M-M elimination pathway for TCPU being incorporated in the model. The M-M kinetics were characterized by maximum rate of elimination (V_{max}) and the Michaelis constant (K_m) for elimination not overall pharmacokinetics.

JPET # 265330

Model with two TMDD components mixing with competitive and non-competitive mechanism (supplemental Figure 2d) :

This model was similar to the model with two TMDD components. The difference lies in the TCPU and TPPU replacement process. In addition to competing with free sEH enzyme, in this model we assumed that TCPU and TPPU also can interact and replace those molecules in the bound drug-sEH complex. TCPU could bind to TPPU-sEH complex with the rate constant $k_{\text{TCPU} \rightarrow \text{TPPU}}$ to release free TPPU and generate TCPU-sEH receptor at the same time. Inversely, TPPU could also bind to TCPU-sEH complexes with a rate constant $k_{\text{TPPU} \rightarrow \text{TCPU}}$ to release free TCPU and generate TPPU-sEH complexes at the same time.

Model with three TMDD components (final model) (Figure 2):

This model was built on top of the model with two TMDD components, with an additional TMDD component for TCPU being incorporated in the model. In this model, both TPPU and TCPU can bind to sEH target (R1). In addition, TCPU can also bind to an unknown target termed a refractory pool (R2) with a different k_{onTCPU} value and dissociate from the TCPU-R2 complex with a different k_{offTCPU} value. We assume the total amount of this unknown target ($R_{\text{max}2}$) in mice is also a constant.

This model was our final model. The equations used to characterize this complicated TMDD model are provide as following:

$$\frac{dA_{\text{TPPU,depot}}}{dt} = -k_{a1} \times A_{\text{TPPU,depot}} \quad (1)$$

$$\frac{dA_{\text{TPPU,central}}}{dt} = k_{a1} \times A_{\text{TPPU,depot}} - k_{\text{on,TPPU,R1}} \times (R_{\text{max}1} - A_{[\text{TPPU-R1}]} + A_{[\text{TCPU-R1}]}) * C_{\text{TPPU,central}} + k_{\text{off,TPPU,R1}} \times A_{[\text{TPPU-R1}]} - k_{e1} \times A_{\text{TPPU,central}}$$

$$A_{\text{TPPU,central}} \quad (2)$$

JPET # 265330

$$\frac{dA_{\text{TCPU,depot}}}{dt} = -k_{a2} \times A_{\text{TCPU,depot}} \quad (3)$$

$$\begin{aligned} \frac{dA_{\text{TCPU,central}}}{dt} = & k_{a2} \times A_{\text{TCPU,depot}} - k_{\text{on,TCPU,R1}} \times (R_{\text{max1}} - A_{[\text{TPPU-R1}]} + A_{[\text{TCPU-R1}]}) \times \\ & C_{\text{TCPU,central}} + k_{\text{off,TCPU,R1}} \times A_{[\text{TCPU-R1}]} - k_{\text{on,TCPU,R2}} \times (R_{\text{max2}} - A_{[\text{TCPU-R2}]}) \times \\ & C_{\text{TCPU,central}} + k_{\text{off,TCPU,R2}} \times A_{[\text{TCPU-R2}]} - k_{e2} \times A_{\text{TCPU,central}} \end{aligned} \quad (4)$$

$$\begin{aligned} \frac{dA_{[\text{TPPU-R1}]}}{dt} = & k_{\text{on,TPPU,R1}} \times (R_{\text{max1}} - A_{[\text{TPPU-R1}]} + A_{[\text{TCPU-R1}]}) \times C_{\text{TPPU,central}} - \\ & k_{\text{off,TPPU,R1}} \times A_{[\text{TPPU-R1}]} \end{aligned} \quad (5)$$

$$\begin{aligned} \frac{dA_{[\text{TCPU-R1}]}}{dt} = & k_{\text{on,TCPU,R1}} \times (R_{\text{max1}} - A_{[\text{TPPU-R1}]} + A_{[\text{TCPU-R1}]}) \times C_{\text{TCPU,central}} - \\ & k_{\text{off,TCPU,R1}} \times A_{[\text{TCPU-R1}]} \end{aligned} \quad (6)$$

$$\begin{aligned} \frac{dA_{[\text{TCPU-R2}]}}{dt} = & k_{\text{on,TCPU,R2}} \times (R_{\text{max2}} - A_{[\text{TCPU-R2}]}) \times C_{\text{TCPU,central}} - k_{\text{off,TCPU,R2}} \times A_{[\text{TCPU-R2}]} \end{aligned} \quad (7)$$

2.2.2 Stochastic models evaluated

Inter-individual variability (IIV): IIV was evaluated using an exponential model which is assumed to be normally distributed with a mean of 0 and a variance of ω^2 .

Residual variability (RV): Additive, proportional and a combined proportional and additive RV models were evaluated. The residual error is assumed to be normally distributed with a mean of 0 and a variance of σ^2 .

2.2.3 Model evaluation

JPET # 265330

Final model selection was based on biological and physiological plausibility, goodness-of-fit plots, individual fitted plots, stability of parameter estimates and objective function value. The likelihood ratio test was used for comparing nested models where a decrease in the NONMEM objective function (-2 log likelihood) of 3.84 points was necessary to consider the improvement in model performance statistically significant at $\alpha = 0.05$.

A visual predictive check (VPC), stratified by TPPU/TCPU and murine strain (WT/KO), was performed to evaluate the predictive ability of the final model. Using the original dataset, along with the final model and its parameter estimates, 1000 virtual observations at each sampling time point were simulated. The observed data were then plotted with the 5th, 50th, and 95th percentiles of the simulated data. If the model is consistent and appropriate, the observed concentrations should fall within the 5th, 50th, and 95th percentiles of the simulated concentrations. The condition (calculated from the ratio of the largest and the smallest eigenvalues) was calculated to evaluate if the model is over-parametrized or ill-conditioned.

2.3 Target occupancy simulation

Target binding kinetics help to evaluate the time of drug action *in vivo*. (de Witte et al., 2016)

The formula of fraction of target occupancy is provided as following

$$\text{Target occupancy} = \frac{\text{The amount of [TPPU-sEH complex]}}{\text{The amount of sEH}} \quad (10)$$

Using the above formula, the fraction of the sEH enzyme that are occupied by TPPU can be estimated. We used our final TMDD model to simulate the time course of fraction of sEH enzyme occupied by TPPU following different doses of TCPU displacement.

JPET # 265330

Simulations were performed in NONMEM (version 7.4.3; ICON Development Solutions, Ellicott City, Maryland) using the structural models detailed in the previous section.

The following conditions were simulated:

1. At time 0, 0.3 mg/kg dose of TPPU was given subcutaneously to the wild-type mice, and at the time 168 hours, 1 mg/kg dose of TCPU was given subcutaneously.
2. At time 0, 0.3 mg/kg dose of TPPU was given subcutaneously to the wild-type mice, and at the time 168 hours, 3 mg/kg dose of TCPU was given subcutaneously.
3. At time 0, 0.3mg/kg dose of TPPU was given subcutaneously to the wild-type mice, and at the time 168 hours, 10 mg/kg dose of TCPU was given subcutaneously.

JPET # 265330

3. RESULTS

In experiment 1, the pharmacokinetics of TPPU has a very long terminal phase in wild-type mice (**Supplemental Figure 3**, middle panel), and this feature was not observed in the sEH knockout mice (**Supplemental Figure 3** top panel), indicating that the binding of TPPU to its pharmacological target sEH affected the disposition of TPPU. In line with this mechanism, a high dose of TCPU given at 168 hr displaced those TPPU molecules bound to sEH, resulting in a TPPU second peak occurred at 170 hr (**Supplemental Figure 3**, bottom panel). These data provided direct and strong evidence that TPPU undergoes pharmacological TMDD. Based on the data from experiment 1, the initial model we built has a TMDD component for TPPU only, with TCPU plasma concentration affecting the k_{off} of TPPU (i.e. dissociation of TPPU). However, this model was unstable and cannot capture the full TCPU dataset, indicating that this is not an appropriate model. Similar to TPPU, TCPU is also a potent sEH inhibitor and therefore its disposition may also be affected by the sEH concentration and distribution. Indeed, as shown in **Figure 3**, when a group of mice receiving a single dose of 3 mg/kg TCPU was administrated with TPPU 2 weeks later, a small TCPU peak was observed shortly after a low dose of TPPU was given, indicating that TPPU can also displace those TCPU bound to sEH. Based on this observation, we updated our model by adding a TMDD component on both TPPU and TCPU (i.e. model with two TMDD components). However, the updated model can characterize TPPU data and TCPU data from the low dose groups (1 mg/kg) but cannot capture the TCPU data from high dose groups (3 and 10 mg/kg). Since a total of 4 different doses of TCPU was evaluated (3 mg/kg from experiment 1 and 0.3, 1, and 10 mg/kg from experiment 2), we evaluated TCPU pharmacokinetics linearity and found that the nonlinearity still existed at the highest dose (i.e. 10 mg/kg) (**Supplemental Figure 4**). Because the capacity of sEH was predicted to be low, the nonlinearity of TCPU observed at

JPET # 265330

high doses cannot be explained by the binding to its low-capacity-high-affinity pharmacological target sEH. To characterize the nonlinearity of TCPU, on top of the model with two TMDD components, we tested additional nonlinear sources of TCPU disposition, such as a M-M elimination pathway or an additional unknown target with large capacity. The different types of models that we have tested, along with their convergence status, model stability, and the objective function values, can be found from the model development history listed in **Supplemental Table 2**. Among the different types of models that we have constructed, the best model was found to be the model with three TMDD components, where TPPU and TCPU compete for their pharmacologic target sEH (R1) with TCPU binding to an additional unknown target pool or refractory pool (R2) with a larger capacity. The model structure of this final model is shown in **Figure 3**.

The final model estimated parameters of TPPU and TCPU pharmacokinetics are presented in **Table 1**. Based on the model estimation, TPPU and TCPU have similar absorption rate constants (0.961 vs 0.730 h⁻¹, respectively), volume of distribution (0.0231 vs 0.0158 L, respectively) and clearance (0.0017 vs 0.0014 L/h, respectively). When TPPU and TCPU competed for sEH binding site, both the association rate constant and dissociate rate constant of TCPU (0.0779 nM⁻¹h⁻¹ and 2.67 h⁻¹, respectively) were similar with that of TPPU (0.0918 nM⁻¹h⁻¹ and 2.24 h⁻¹, respectively). The binding of TCPU to the unknown target is much weaker, as reflected by the smaller k_{on} of 0.0275 nM⁻¹h⁻¹ and large k_{off} of 11.9 h⁻¹. The capacity of sEH (R_{max1}) and the unknown target (R_{max2}) were estimated to be 16.2 nmol and 46.6 nmol, respectively. In the final model, IIV terms were placed on the volume distribution, clearance and absorption rate constant of TPPU and TCPU; a combined proportional and additive residual error model best described the unexplained residual variability. Inter-individual variability estimates (ETAs) on V, CL and k_a of TPPU and

JPET # 265330

TCPU can be found from **Table 1**. The calculated shrinkage for etas in the final model ranges from 2% to 67%. Shrinkage above 30% may influence the power of the diagnostics for individual predicted parameters and concentrations. However, removing the IIV on V , k_a and k_{off} of TCPU negatively impact the model stability and fit. Condition number (calculated from the ratio of the largest and the smallest eigenvalues) of the final model is 161. Since this value is less than 1000, it indicates that the model is not over-parametrized or ill-conditioned.

To further evaluate the model performance, the model predicted TPPU and TCPU parameters, including C_{max} , AUC_{inf} , and $t_{1/2}$, were compared with those obtained from noncompartmental analysis (NCA) using the observed data. As shown in **Table 2**, the model predicted values are in line with those from the NCA. In addition, the model predicted k_{off} as well as the capacity of sEH (i.e. R_{max1}) were also consistent with the experimental determine values (**Table 2**)

The standard goodness-of-fit plot of the final model for TPPU and TCPU are shown in **Figure 4a and Figure 4b**, respectively. The population- and individual- predicted concentrations versus the observed concentrations were evenly distributed around the line of identity without bias, indicating that the final model characterized both TPPU and TCPU pharmacokinetics adequately at both the population and individual levels. Additionally, the conditional weighted residuals appear distributed uniformly around the zero line when plotted either by population-predicted concentrations or by time, further indicating the absence of significant bias in the model fit.

The time course of mean observed versus population-predicted (PRED) plasma concentrations of TPPU and TCPU are presented in **Figures 5-7**. As shown in **Figure 5**, the final model was able to adequately characterize TPPU pharmacokinetics in both sEH knockout mice (top panel) and wild-type mice without or with TCPU displacement (middle panel and bottle panel, respectively) simultaneously. This model also captured the dose-dependent displacement effect of TCPU on

JPET # 265330

TPPU pharmacokinetics, which is reflected by the higher 2nd peak of TPPU with increase in TCPU dose (**Figure 6**). In addition, the final model also provided favorable fitting on TCPU pharmacokinetics following different TCPU doses (**Figure 7**). To evaluate the predictive ability of the final model, VPC was performed. As shown in **Supplemental Figure 5**, the solid lines, depicting the 2.5th, 50th, and 97.5th percentiles of the predicted TPPU and TCPU concentrations, cover most of the observed data and also in close agreement with the 2.5th, 50th, and 97.5th percentiles of the observed data, confirming the adequacy of the final model.

The simulation result for the time course of sEH target occupancy (TO) for TPPU with different doses of TCPU displacement is shown in the **Figure 8**. Following 0.3 mg/kg TPPU, sEH occupancy reaches 90% shortly after TPPU administration and starts to decline after 24 hr. Based on the simulation, about 40% of sEH is still bound with TPPU after 7 days. The fraction of sEH occupied by TPPU drops dramatically shortly after TCPU is administered and it happens in a dose dependent manner, indicating the target displacement by TCPU.

JPET # 265330

4. DISCUSSION

TMDD is a term to describe the phenomenon where the interaction between drug and its pharmacologic target, a pharmacodynamics process, affects drug disposition, a pharmacokinetics process. Although the concept of TMDD was raised by Levy 25 years ago based on the unusual nonlinear pharmacokinetics of a number of small-molecule drugs, TMDD only became a widely-known concept with the proliferation of large-molecule biologics because numerous protein drugs demonstrate nonlinear pharmacokinetics imparted by TMDD due to their specific binding to their pharmacological targets (Levy, 1994; Dua et al., 2015). Due to the relatively low prevalence of TMDD in small-molecule drugs, it has been an overlooked area (An, 2017; van Waterschoot et al., 2018), misunderstanding has evolved that “TMDD cannot occur in small-molecule compounds”. This is a clear misconception and our study has provided direct evidence that TMDD can occur in small-molecule compounds. To verify the occurrence of pharmacological TMDD, a number of mechanism experiments have been recommended, including pharmacokinetic experiment using pharmacological target knock-out animals as well as *in vivo* displacement experiment with co-administration of pharmacological target binding displacer (Veng-Pedersen et al., 1997; Retlich et al., 2009; An, 2017; An, 2020). So far only a few groups have done such mechanism experiments to verify TMDD in large-molecule and small-molecule compounds but none of them have done both experiments within the same study (Veng-Pedersen et al., 1997; Retlich et al., 2009) Both recommended experiments have been performed in our study, which represent an advantage of our work. Our observations of long terminal phase of TPPU in wild-type mice while not in sEH-knockout mice, along with the occurrence of second TPPU peak following administration of TCPU provide clear and direct evidence of pharmacological TMDD of TPPU, a potent small-molecule sEH inhibitor.

JPET # 265330

Based on the TPPU and TCPU pharmacokinetics data from both mechanism experiments, we developed a novel simultaneous TMDD interaction model, where TPPU and TCPU compete for their pharmacologic target sEH. Based on our final model, the total amount of sEH enzyme (R_{max1}) in mice was predicted to be around 16.2 nmol, which is consistent with the experimental value of 10 nmol (Lee et al., 2019). The dissociation rate constants (k_{off}) of TPPU and TCPU were predicted to be 2.24 h^{-1} and 2.67 h^{-1} , respectively, which is close to the values (2.09 h^{-1} and 1.76 h^{-1} , respectively) obtained from the *in vitro* experiment. Regarding the K_d predicted by pharmacokinetic model, which is calculated by k_{off} over k_{on} , were predicted to be 24.4 nM for TPPU and 34.3 nM for TCPU. These estimates are higher than those experimentally determined K_d values (2.5 nM for TPPU and 0.92 nM for TCPU) (Lee et al., 2019). This discrepancy is not surprising since K_d values determined *in vitro* is usually measured in a closed system which is different from the *in vivo* situation where a drug is exposed to an open system. Recently, a number of studies have suggested that drug-target residence time (t_R), which is calculated as $1/k_{off}$, is a better *in vitro* parameter to predict *in vivo* efficacy than those standard *in vitro* potency parameters, including K_d (Copeland, 2016; Lee et al., 2019). Our model results indirectly support this recommendation considering that the k_{off} values determined *in vitro* are consistent with those estimated from the mathematical modeling using the *in vivo* data, while the K_d values determined *in vitro* are much smaller than the model predicted values. The disconnection between model predicted and *in vitro* determined K_d has been reported before for other compounds (Dua et al., 2015). Although TMDD models have been well documented, most of them were established in a single compound scenario. Our novel model represents the first TMDD interaction model for small-molecule compounds.

JPET # 265330

In our final TMDD interaction model, in addition to TPPU and TCPU competing for sEH enzyme, TCPU was predicted to bind to an additional target pool. Based on the model prediction, the capacity of this unknown target is 46.6 nmol, which is higher than sEH (16.2 nmol). In addition, TCPU was predicted to be dissociated from this target with k_{off} value of 11.9 h⁻¹, which is much faster than its dissociation from sEH. We anticipate that TCPU has specific binding to this unknown target as a second TMDD component for TCPU is required in the model in order to capture TCPU nonlinear pharmacokinetics observed in our experiment. It would be interesting to know what this unknown target is. In addition to sEH, many other epoxide hydrolase isozymes, including mEH, EH3, EH4, are known to be expressed in mammals. These isozymes share the similar protein structure with sEH enzyme with similar hydrolysis activity but different tissue expression and substrate preferences (Decker et al., 2009). Theoretically, if TCPU has broad inhibitory effect on epoxide hydrolase isozymes, then this model predicted second target pool could be one of these isozymes. TCPU has potent inhibitory effect on sEH. Whether TCPU has inhibitory effect on other epoxide hydrolase isozymes or other unknown targets warrants further investigation.

As noted earlier, TMDD is a consequence of PD affecting pharmacokinetics. Accordingly, for compounds exhibiting TMDD, valuable information on drug binding to its pharmacological target can be extracted from the observed pharmacokinetics profile. For the TMDD interaction model that we developed for TPPU and TCPU, it can be used not only for pharmacokinetics characterization but also for sEH target occupancy prediction. Our simulation result predicted that, 90% of the sEH will be occupied shortly after a low dose of 0.3 mg/kg TPPU administration, with $\geq 40\%$ of sEH remaining bound with TPPU for at least 7 days. If sEH target occupancy is directly correlated with the pharmacodynamics effect, then long-lasting efficacy is expected following a

JPET # 265330

single dose of TPPU. Further efficacy experiments are warranted to confirm the predicted target occupancy.

Changes in the magnitude and time course of TPPU/TCPU exposure and drug action in tissues of interest other than blood are also required to be investigated. Physiologically based pharmacokinetic (PBPK) model is commonly used to integrate the system components (e.g. body fluid dynamics, tissue size and composition, abundance and distribution of drug receptors, and membrane transporters in various organ and tissue compartments) and the drug-dependent component to enables the study of ADME processes and mechanisms of action at the cellular level (Zhao et al., 2011). Our long-term goal is to use TPPU as a model drug to build a PBPK-TMDD model to better describe the pharmacokinetics and target occupancy of sEH inhibitors, which could facilitate the drug design of sEH inhibitors and clinical dosage regime design of those small molecule drugs with strong TMDD characteristics.

JPET # 265330

ACKNOWLEDGEMENT

This work is partially supported by National Institute of Health National Institute of Environmental Health Sciences [Grants ES004699, ES030443, and ES024806].

JPET # 265330

AUTHORSHIP CONTRIBUTIONS

- Participated in research design: Hammock, Lee
- Conducted experiments: Hammock, Lee
- Contributed new reagents or analytic tools: Hammock, Lee
- Performed data analysis: Wu, An
- Wrote or contributed to the writing of the manuscript: An, Wu, Hammock, Lee

JPET # 265330

REFERENCES

- Ait-Oudhia S, Scherrmann J-M and Krzyzanski W (2010) Simultaneous pharmacokinetics/pharmacodynamics modeling of recombinant human erythropoietin upon multiple intravenous dosing in rats. *Journal of Pharmacology and Experimental Therapeutics* **334**:897-910.
- An G (2017) Small - Molecule Compounds Exhibiting Target - Mediated Drug Disposition (TMDD): A Minireview. *The Journal of Clinical Pharmacology* **57**:137-150.
- An G (2020) Concept of Pharmacologic Target-Mediated Drug Disposition in Large-Molecule and Small-Molecule Compounds. *J Clin Pharmacol* **60**:149-163.
- Copeland RA (2016) Drug-target interaction kinetics: underutilized in drug optimization? *Future Med Chem* **8**:2173-2175.
- de Witte WE, Danhof M, van der Graaf PH and de Lange EC (2016) In vivo target residence time and kinetic selectivity: the association rate constant as determinant. *Trends in pharmacological sciences* **37**:831-842.
- Decker M, Arand M and Cronin A (2009) Mammalian epoxide hydrolases in xenobiotic metabolism and signalling. *Archives of toxicology* **83**:297-318.
- Dua P, Hawkins E and Van der Graaf P (2015) A tutorial on target - mediated drug disposition (TMDD) models. *CPT: pharmacometrics & systems pharmacology* **4**:324-337.
- Gibiansky L and Gibiansky E (2010) Target-mediated drug disposition model for drugs that bind to more than one target. *Journal of pharmacokinetics and pharmacodynamics* **37**:323-346.
- Goswami SK, Wan D, Yang J, Da Silva CAT, Morisseau C, Kodani SD, Yang G-Y, Inceoglu B and Hammock BD (2016) Anti-ulcer efficacy of soluble epoxide hydrolase inhibitor TPPU on diclofenac-induced intestinal ulcers. *Journal of Pharmacology and Experimental Therapeutics* **357**:529-536.
- Grimm HP (2009) Gaining insights into the consequences of target-mediated drug disposition of monoclonal antibodies using quasi-steady-state approximations. *Journal of pharmacokinetics and pharmacodynamics* **36**:407.
- Guo Y, Luo F, Zhang X, Chen J, Shen L, Zhu Y and Xu D (2018) TPPU enhanced exercise - induced epoxyeicosatrienoic acid concentrations to exert cardioprotection in mice after myocardial infarction. *Journal of cellular and molecular medicine* **22**:1489-1500.
- Lee KSS, Liu J-Y, Wagner KM, Pakhomova S, Dong H, Morisseau C, Fu SH, Yang J, Wang P and Ulu A (2014) Optimized inhibitors of soluble epoxide hydrolase improve in vitro target residence time and in vivo efficacy. *Journal of medicinal chemistry* **57**:7016-7030.
- Lee KSS, Morisseau C, Yang J, Wang P, Hwang SH and Hammock BD (2013) Förster resonance energy transfer competitive displacement assay for human soluble epoxide hydrolase. *Analytical biochemistry* **434**:259-268.
- Lee KSS, Yang J, Niu J, Ng CJ, Wagner KM, Dong H, Kodani SD, Wan D, Morisseau C and Hammock BD (2019) Drug-Target Residence Time Affects in Vivo Target Occupancy through Multiple Pathways. *ACS central science*.
- Levy G (1994) Pharmacologic target - mediated drug disposition. *Clinical Pharmacology & Therapeutics* **56**:248-252.
- Liu J, Lin Y-P, Morisseau C, Lee KSS, Rose TE, Hwang SH and Hammock BD (2012) Substituted phenyl groups improve the pharmacokinetic profile of urea-based soluble epoxide hydrolase inhibitors, in, Federation of American Societies for Experimental Biology.
- Mager DE and Jusko WJ (2001) General pharmacokinetic model for drugs exhibiting target-mediated drug disposition. *Journal of pharmacokinetics and pharmacodynamics* **28**:507-532.

JPET # 265330

- Ostermann AI, Herbers J, Willenberg I, Chen R, Hwang SH, Greite R, Morisseau C, Gueler F, Hammock BD and Schebb NH (2015) Oral treatment of rodents with soluble epoxide hydrolase inhibitor 1-(1-propanoylpiperidin-4-yl)-3-[4-(trifluoromethoxy) phenyl] urea (TPPU): Resulting drug levels and modulation of oxylipin pattern. *Prostaglandins & other lipid mediators* **121**:131-137.
- Retlich S, Withopf B, Greischel A, Staab A, Jaehde U and Fuchs H (2009) Binding to dipeptidyl peptidase - 4 determines the disposition of linagliptin (BI 1356) – investigations in DPP - 4 deficient and wildtype rats. *Biopharmaceutics & drug disposition* **30**:422-436.
- Tu R, Armstrong J, Lee KSS, Hammock BD, Sapirstein A and Koehler RC (2018) Soluble epoxide hydrolase inhibition decreases reperfusion injury after focal cerebral ischemia. *Scientific reports* **8**:5279.
- van Waterschoot RA, Parrott NJ, Olivares-Morales A, Lavé T, Rowland M and Smith DA (2018) Impact of target interactions on small-molecule drug disposition: an overlooked area. *Nature Reviews Drug Discovery* **17**:299.
- Veng-Pedersen P, Widness J, Wang J and Schmidt R (1997) A tracer interaction method for nonlinear pharmacokinetics analysis: application to evaluation of nonlinear elimination. *Journal of pharmacokinetics and biopharmaceutics* **25**:569-593.
- Wagner KM, McReynolds CB, Schmidt WK and Hammock BD (2017) Soluble epoxide hydrolase as a therapeutic target for pain, inflammatory and neurodegenerative diseases. *Pharmacology & therapeutics* **180**:62-76.
- Yan X, Chen Y and Krzyzanski W (2012) Methods of solving rapid binding target-mediated drug disposition model for two drugs competing for the same receptor. *Journal of pharmacokinetics and pharmacodynamics* **39**:543-560.
- Yao E-s, Tang Y, Liu X-h and Wang M-h (2016) TPPU protects tau from H₂O₂-induced hyperphosphorylation in HEK293/tau cells by regulating PI3K/AKT/GSK-3 β pathway. *Journal of Huazhong University of Science and Technology [Medical Sciences]* **36**:785-790.
- Zhao P, Zhang L, Grillo J, Liu Q, Bullock J, Moon Y, Song P, Brar S, Madabushi R and Wu T (2011) Applications of physiologically based pharmacokinetic (PBPK) modeling and simulation during regulatory review. *Clinical Pharmacology & Therapeutics* **89**:259-267.

JPET # 265330

FIGURE LEGENDS

Figure 1. Schematic flow diagram of animal study protocol in experiment 1 and experiment 2. Four treatment groups from wild-type or sEH-deficiency mice were included in experiment 1. Three treatment groups from wild-type mice were included in experiment 2.

Figure 2. Final TMDD model describing the pharmacokinetics of TPPU and TCPU. Both TPPU and TCPU were absorbed from the depot with first-order absorption rate constants (k_{a1} , and k_{a2} , respectively) and eliminated from the central compartment with first-order elimination rate constants (k_{e1} , and k_{e2} , respectively). Both TPPU and TCPU can bind with sEH (i.e. R1) with second-order association rate constant ($k_{on,TPPU,R1}$ and $k_{on,TCPU,R1}$, respectively) to form drug-sEH complexes. TPPU-sEH and TCPU-sEH can dissociate back to free drug and free sEH target with the first-order dissociation rate constants ($k_{off,TPPU,R1}$ and $k_{off,TCPU,R1}$, respectively). In addition, TCPU can also bind to an unknown target termed a refractory pool (R_2) with a different $k_{on,TCPU,R2}$ value and dissociate from the TCPU- R_2 complex with a different $k_{off,TCPU,R2}$ value. The total amount of sEH (R_{max1}) and refractory pool (R_{max2}) in mice are assumed to be constant.

Figure 3. Time courses of the mean observed TPPU and TCPU plasma concentrations in wild-type mice following 0.3 mg/kg TPPU at time 0 and 0.3 mg/kg TCPU at time 168 hours. The mice used in this experiment were reused from a previous experiment, where the mice were given a weak sEH inhibitor, mTPPU, at 1 mg/kg s.c 3 weeks ago followed by 3mg/kg TCPU s.c. one weeks from the administration of mTPPU.

Figure 4. Goodness fit plots for the final population pharmacokinetics modeling for : a) TPPU observed versus population-predicted b) TPPU observed versus individual-predicted; c) TCPU

JPET # 265330

observed versus population-predicted, and d) TCPU observed versus individual-predicted; Solid black lines represent the lines of identity. Solid blue lines represent lowessline

Figure 5. Time courses of mean observed (symbols) and model predicted (lines) TPPU plasma concentrations following 0.3 mg/kg TPPU at time 0 in a) sEH deficient mice without TCPU displacement; b) wild-type mice without TCPU displacement; and c) wild-type mice with 3 mg/kg TCPU displacement at 168 hours.

Figure 6. Time courses of mean observed (symbols) and model predicted (lines) TPPU plasma concentrations when wild-type mice received 0.3 mg/kg TPPU at time 0 and different doses of TCPU (1 or 10 mg/kg) at 168 hours (N=6 per group)

Figure 7. Time courses of mean observed (symbols) and model predicted (lines) TCPU plasma concentrations when wild-type mice received 0.3 mg/kg TPPU at time 0 and different doses of TCPU (1, 3, or 10 mg/kg) at 168 hours (N=6 per group).

Figure 8. Simulated time course of fraction of sEH occupied by TPPU when wild-type mice receive 0.3 mg/kg TPPU at time 0 and different doses of TCPU (1, 3, or 10 mg/kg) at 168 hours.

JPET # 265330

Table1. Estimated parameters from the final TMDD model

Parameters (unit)	Definition	Estimate	%RSE	Shrinkage
$V_2(L)$	TPPU central volume of distribution	0.0231	13	
$V_4(L)$	TCPU central volume of distribution	0.0158	18	
$CL_2(L/h)$	TPPU clearance	0.0017	8	
$CL_4(L/h)$	TCPU clearance	0.0014	17	
$KA_1(h^{-1})$	TPPU first-order absorption rate constant	0.961	10	
$KA_3(h^{-1})$	TCPU first-order absorption rate constant	0.73	12	
$k_{on\ TPPU, R1}(nM^{-1}h^{-1})$	TPPU second-order association rate constant to sEH	0.0918	20	
$k_{off\ TPPU, R1}(h^{-1})$	TPPU first-order dissociation rate constant from sEH	2.24	20	
$k_{on\ TCPU, R1}(nM^{-1}h^{-1})$	TCPU second-order association rate constant to sEH	0.0779	44	
$k_{off\ TCPU, R1}(h^{-1})$	TCPU first-order dissociation rate constant from sEH	2.67	91	
$k_{on\ TCPU, R2}(nM^{-1}h^{-1})$	TCPU second-order association rate constant to unknown receptor	0.0275	96	
$k_{off\ TCPU, R2}(h^{-1})$	TCPU first-order dissociation rate constant from unknown receptor	11.9	92	
$R_{max1}(nmol)$	total sEH amount	16.2	4	
$R_{max2}(nmol)$	total unknown receptor amount	46.6	20	
ω^2_{V2}	variance of inter-individual variability on V_2	0.353	31	5
ω^2_{V4}	variance of inter-individual variability on V_4	0.178	42	35
ω^2_{cl2}	variance of inter-individual variability on V_2	0.17	46	2
ω^2_{cl4}	variance of inter-individual variability on V_2	0.315	36	28
ω^2_{ka1}	variance of inter-individual variability on V_2	0.195	42	9
ω^2_{ka3}	variance of inter-individual variability on V_2	0.0459	55	46
$\omega^2_{koff, TCPU, R1}$	variance of inter-individual variability on V_2	3.74	60	42
$\omega^2_{koff, TCPU, R2}$	variance of inter-individual variability on V_2	0.31	121	67
σ_1^2	Proportional variance of residual variability of TPPU	0.083	15	11
σ_2^2	Proportional variance of residual variability of TCPU	0.0557	38	17
σ_3^2	Additive variance of residual variability of TPPU	18.5	52	11
σ_4^2	Additive variance of residual variability of TCPU	0.0381	14	17

Condition number:161

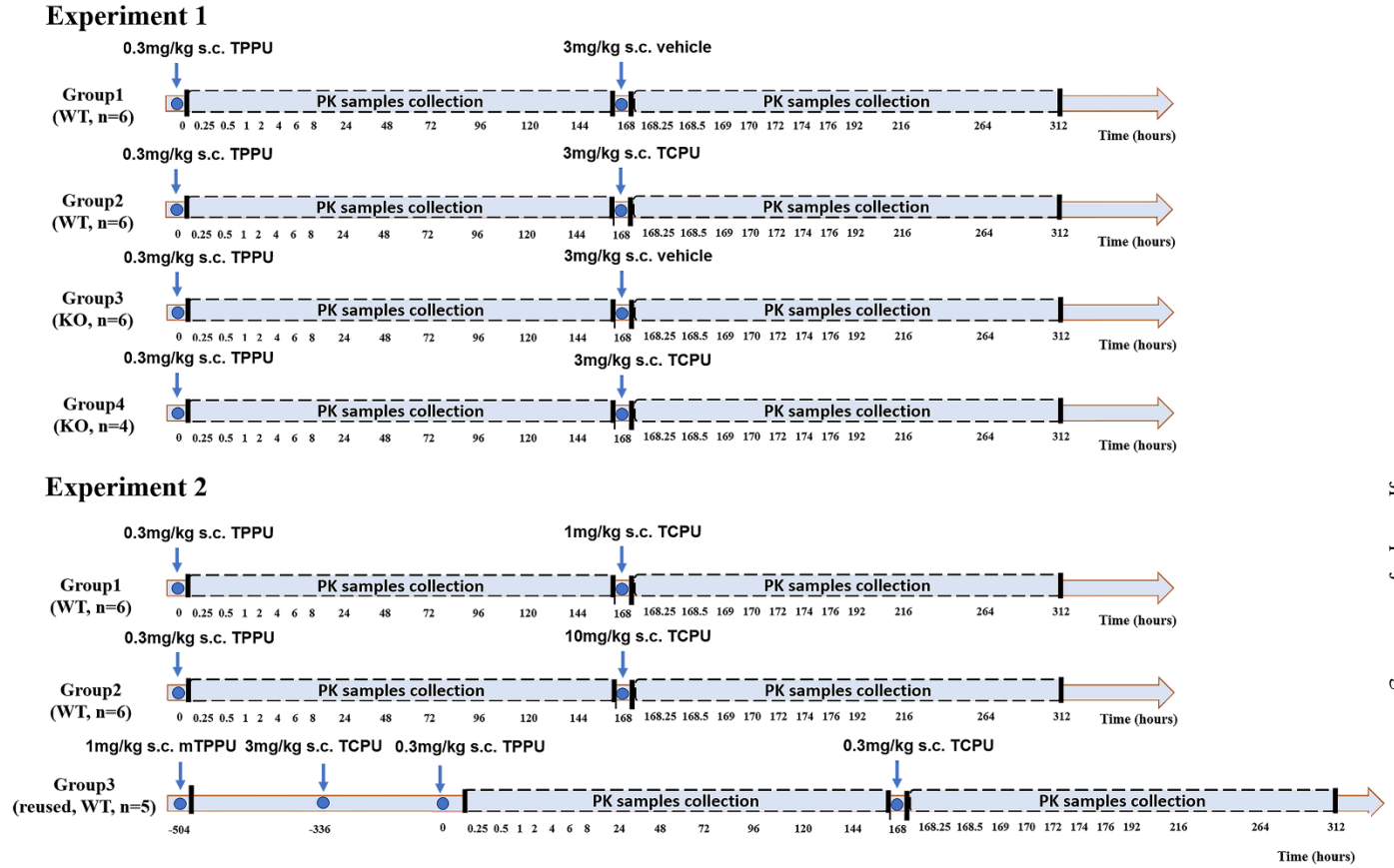
Table2. Parameters comparison between observed and predicted values.

Compound	Dose (mg/kg)	C _{max} (nM)		AUC _{inf} (nM*h)		t _{1/2} (h)		k _{off} (h ⁻¹)		sEH _{total} (nmol)	
		Observed	Predicted	Observed	Predicted	Observed	Predicted	Observed	Predicted	Observed	Predicted
TPPU	0.3	436±319	390±250	12100±4630	12700±3360	54.3±17.5	58.6±9.33	2.09	2.24		
								(Lee et al., 2013)			10.0
TCPU	1.0	853±207	971±196	22800±3720	21900±3340	15.2±2.64	16.3±1.68	1.76	2.67	(Lee et al., 2019)	
	3.0	9220±2940	8740±3150	159000±17800	144000±33400	10.5±4.67	11.6±2.15	(Lee et al., 2013)			
	10.0	57300±11600	49800±9570	1200000±85500	102000±162000	11.6±0.86	11.7±0.56				

data are presented as mean ± SD.

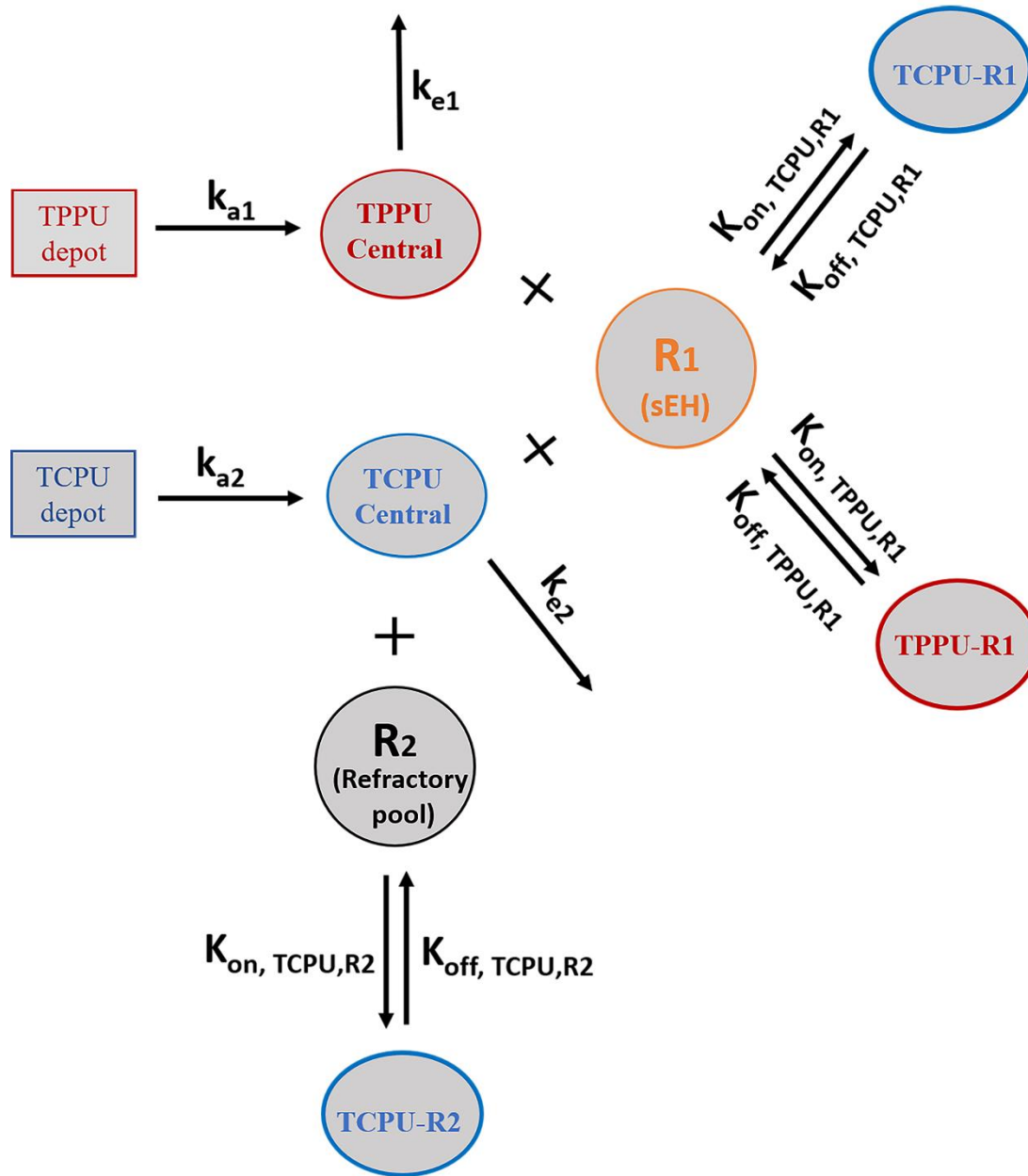
k_{off}, first-order dissociation rate constant; AUC_{inf}, area under the concentration-time curve from predose extrapolated to infinity; C_{max}, maximum concentration, t_{1/2}, terminal elimination half-life; sEH_{total}, sEH total amount in rat body.

Figure 1



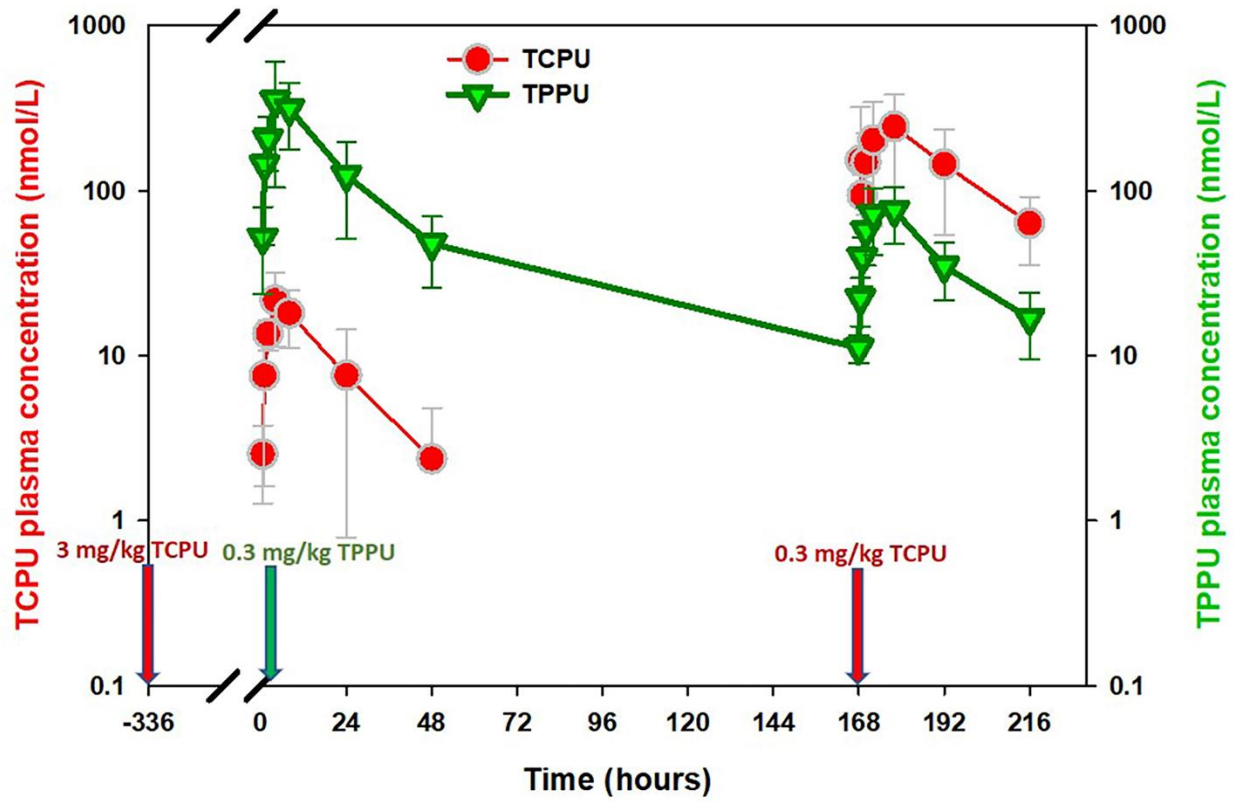
JPET # 265330

Figure 2



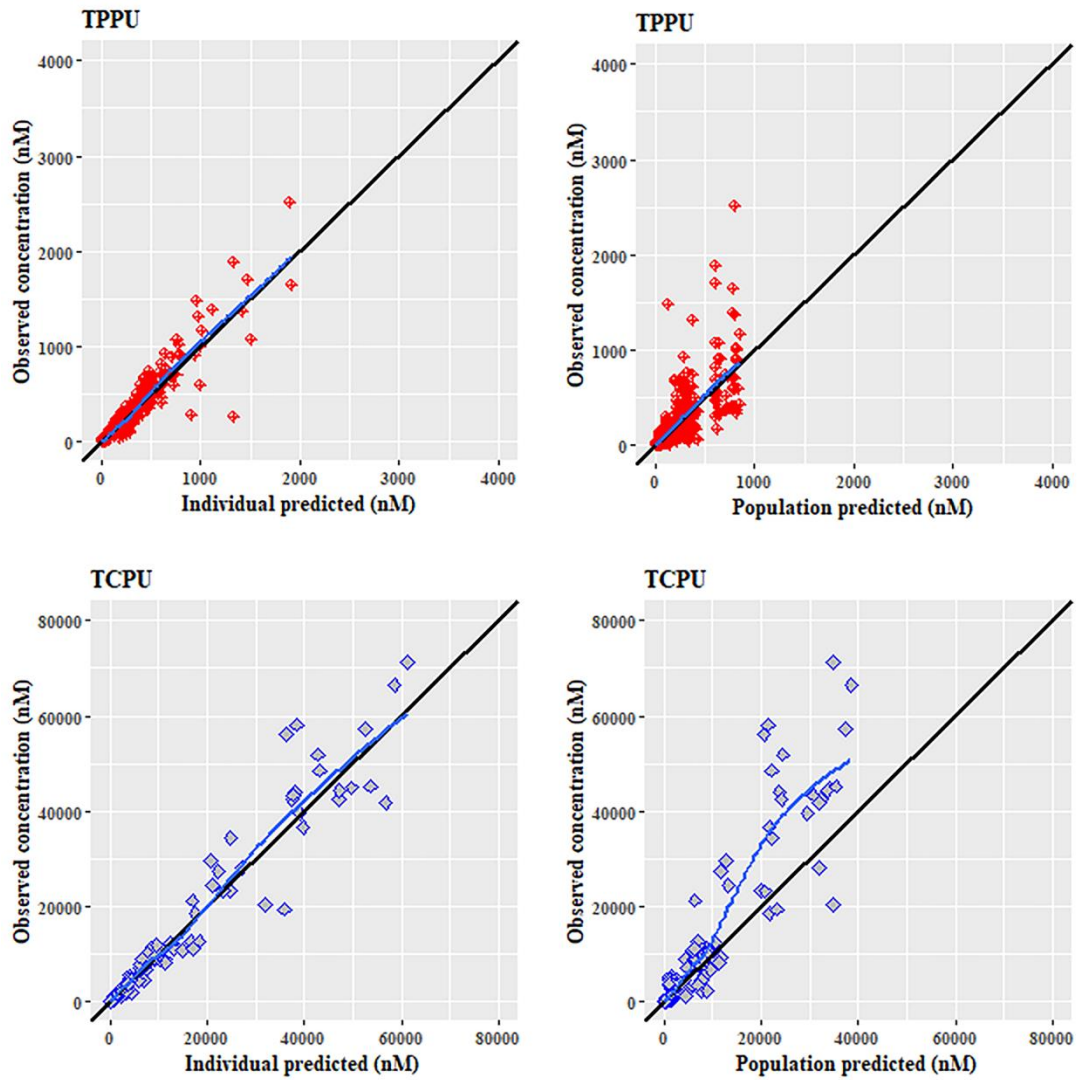
JPET # 265330

Figure 3



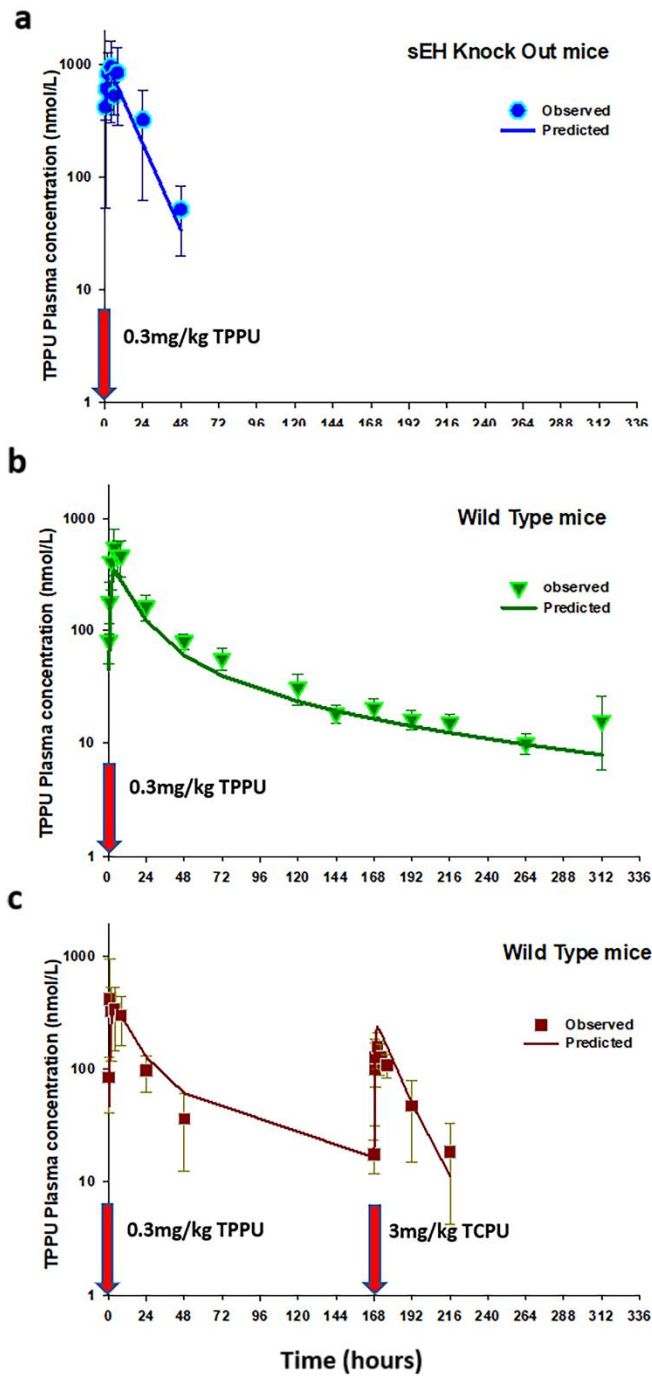
JPET # 265330

Figure 4



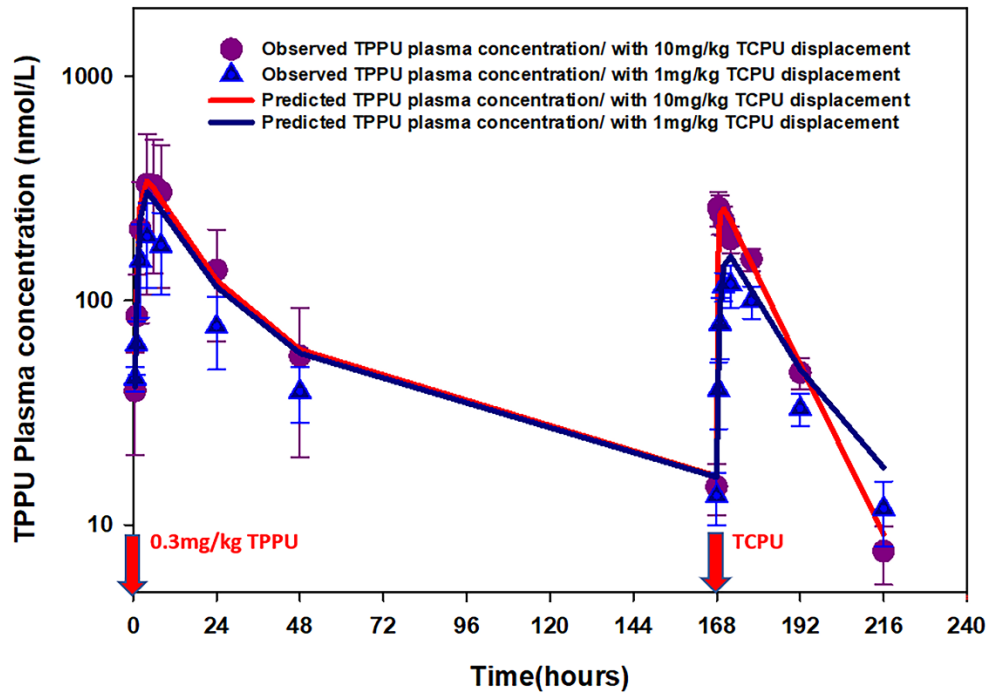
JPET # 265330

Figure 5



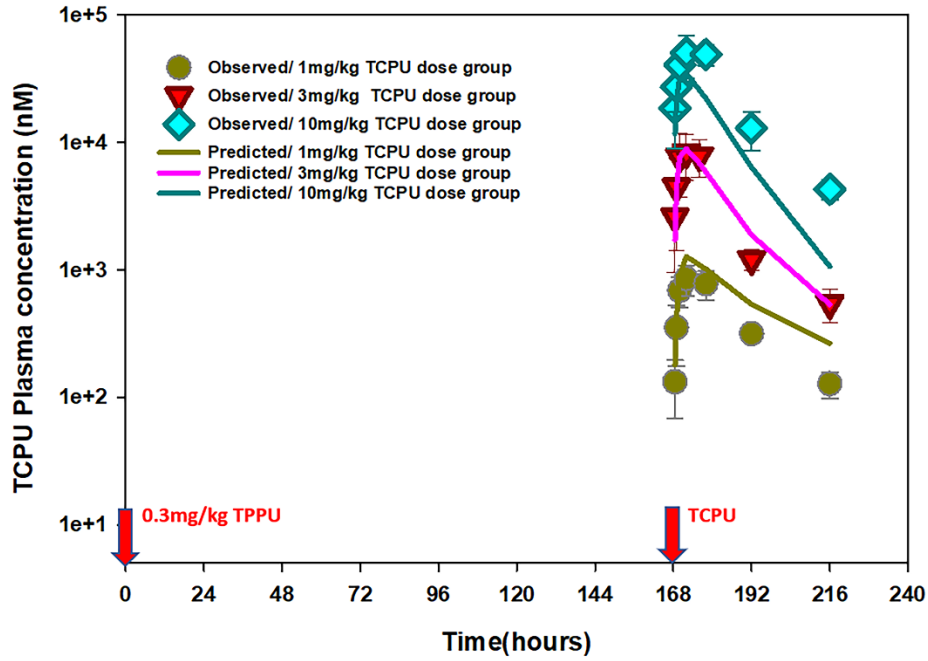
JPET # 265330

Figure 6



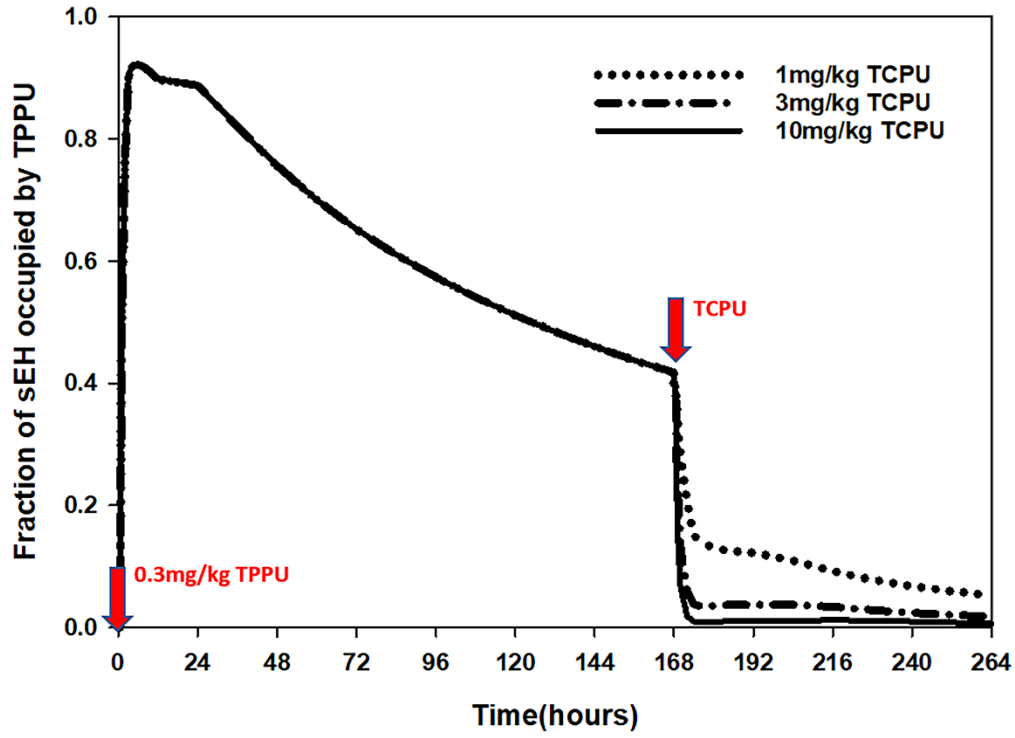
JPET # 265330

Figure 7.



JPET # 265330

Figure 8



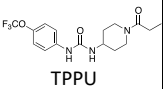
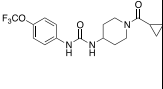
JPET # 265330

**Simultaneous Target-Mediated Drug Disposition (TMDD) Model for Two
Small-Molecule Compounds Competing for Their Pharmacological Target:
Soluble Epoxide Hydrolase**

Nan Wu, Bruce D. Hammock, Kin Sing Stephen Lee, Guohua An

The Journal of Pharmacology and Experimental Therapeutics

Supplemental Table 1. Physical properties and human, mouse, and rat kinetics parameters of TPPU and TCPU. (Liu et al., 2012; Lee et al., 2013; Lee et al., 2014; Lee et al., 2019)

Structure	Physical Properties				Human								Mouse		Rat	
	Mol. Weight	Sol ^c (ug/mL)	Melting Point (°C)	Log P	IC ₅₀ (nM) (sEH)	K _i (nM) (sEH)	IC ₅₀ (nM) sEH tDPP O	k _{off} / t _{1/2} (x10 ⁻⁴ s ⁻¹ / min) (sEH) ^d	HERG Inhibition at 50 μM (%)	Plasma Protein Binding at 1μM (%)	CYP 2J Remaining activity at 10 μM (%)	CYP2C Remaining activity at 10 μM (%)	K _i (nM) (sEH)	k _{off} / t _{1/2} (x10 ⁻⁴ s ⁻¹ / min) (sEH) ^d	IC ₅₀ (nM) (sEH)	k _{off} / t _{1/2} (x10 ⁻⁴ s ⁻¹ / min) (sEH) ^d
 TPPU	359.34	60	198.2-200.8 (199.5)	3.23	3.7	0.64±0.09 0.91±0.13	34	10.5±0.2/ 11.0±0.2	26±1	79±1	91.9±2.2	118±2.4	2.50±0.38	5.84±0.05/ 19.8±0.2	29.1±4.5	8.52±0.47/ 13.6±0.8
 TCPU	371.35	4.6	193.4-194.2 (193.8)	3.28	2	0.55±0.10	20.3	6.67±0.45/ 17.4±1.2		90.0±0.5			0.92±0.09	4.89±0.54/ 23.8±2.7	9.9±0.1	7.30±0.55/ 15.89±1.21

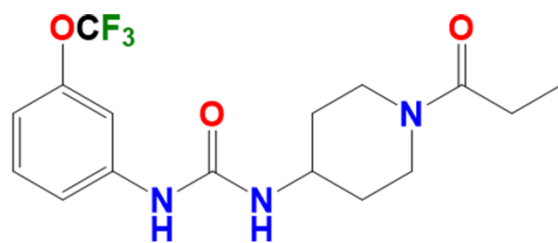
Supplemental Table2. Model building history

No.	Dataset	Description	Model fit process	OFV
1	Data only from experiment 1	5 compartmental model; Only TPPU shows TMDD; TPPU k_{off} was affected by TCPU plasma concentration;	Minimization successfully; Fit well with high RSE	3013.497
2	Data only from group experiment 1	6 compartmental model; TPPU and TCPU both show TMDD binding with R1 competitively;	Minimization successfully; Fit well with high RSE	2992.667
3	Data from group experiment 1 and 2 (experiment 2 group 3 was excluded)	6 compartmental model; TPPU and TCPU both show TMDD binding with R1 competitively;	Minimization successfully; Did not capture TCPU high dose	5811.443
4	Data from group experiment 1 and 2 (experiment 2 group 3 was excluded)	7 compartmental model; TPPU and TCPU both show TMDD binding with R1 competitively; TCPU and TPPU could also bind with each other's receptor complex; TCPU has another specific binding pool R2;	Terminated	
5	Data from group experiment 1 and 2 (experiment 2 group 3 was excluded)	6 compartmental model; TPPU and TCPU both show TMDD binding with R1 competitively; TCPU and TPPU could also bind with each other's receptor complex;	Terminated	
6	Data from group experiment 1 and 2 (experiment 2 group 3 was excluded)	7 compartmental model; TPPU and TCPU both show TMDD binding with R1 competitively; TCPU has peripheral compartment;	Minimization successfully; Did not capture TCPU high dose with high RSE	5770.227

7	Data from group experiment 1 and 2 (experiment 2 group 3 was excluded)	6 compartmental model; TPPU and TCPU both show TMDD binding with R1 competitively; TCPU also have M-M elimination;	Minimization successfully; Fit well with high RSE	5921.653
8	Data from group experiment 1 and 2	7 compartmental model; TPPU and TCPU both show TMDD binding with R1 competitively; TCPU has another specific binding pool R2;	Minimization successfully; Did not capture TCPU high dose with high RSE	6227.922
Final Model	Data from group experiment 1 and 2 (experiment 2 group 3 was excluded)	7 compartmental model; TPPU and TCPU both show TMDD binding with R1 competitively; TCPU has another specific binding pool R2;	Minimization successfully; Good	5744.069

OFV, objective function value; RSE, relative standard errors.

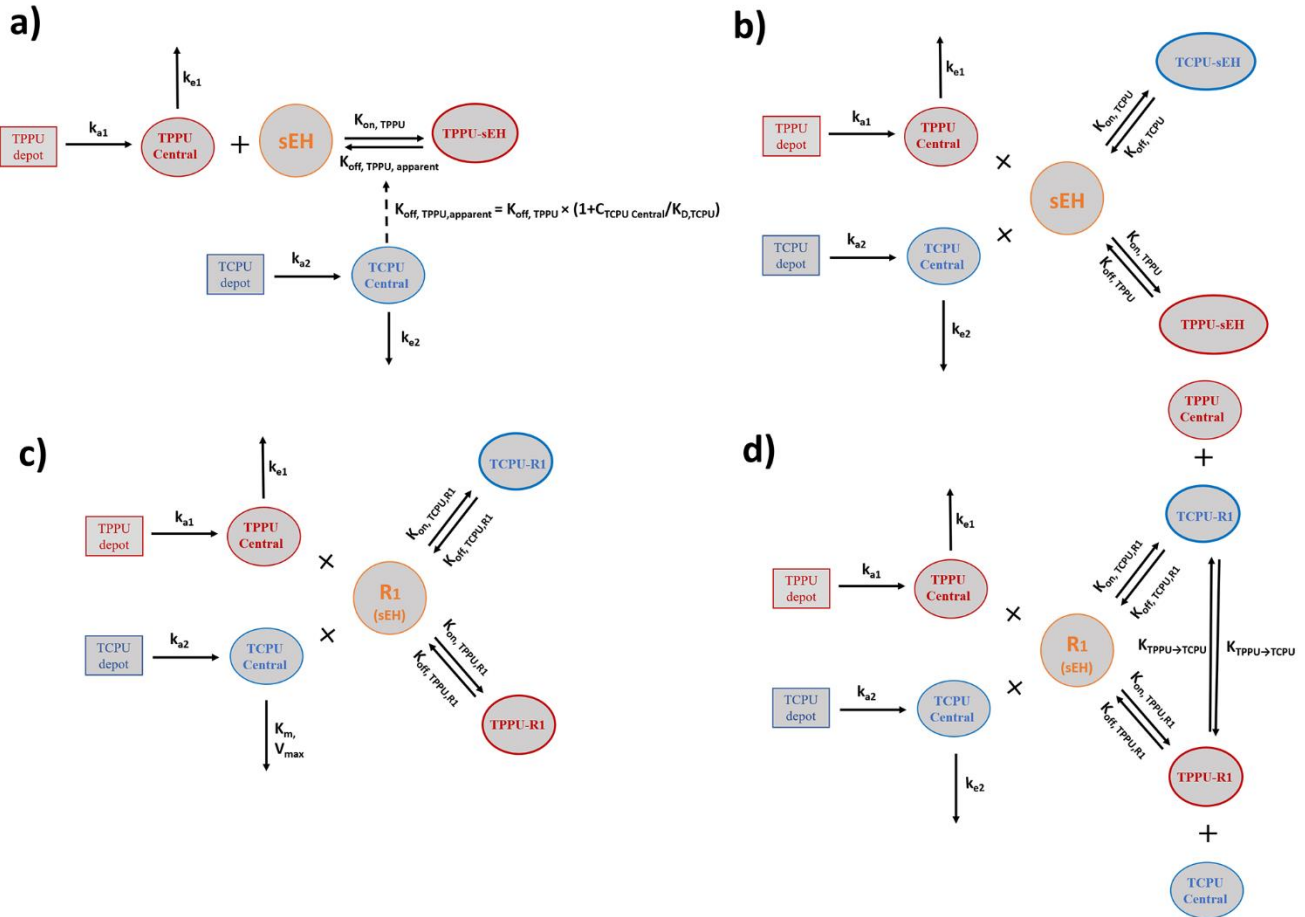
Supplemental Figure 1. Chemical structure of mTPPU.



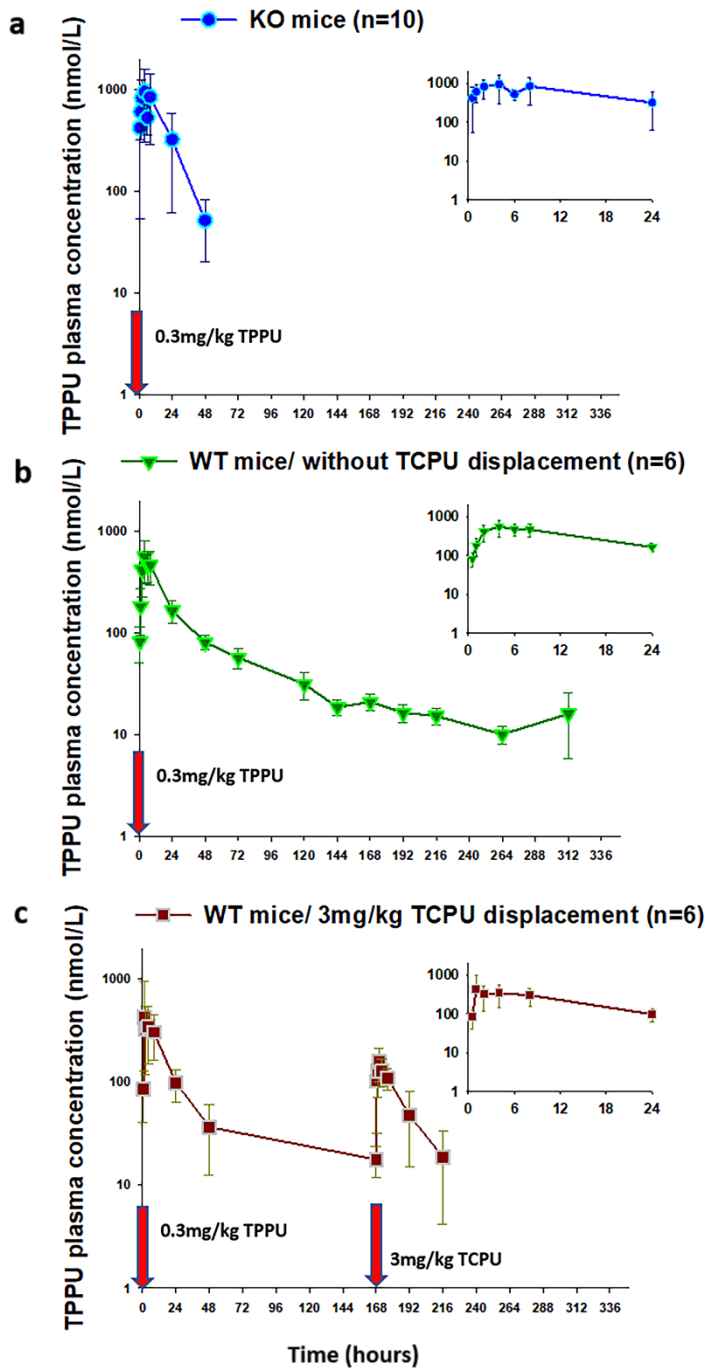
mTPPU

3-(3-trifluoromethoxy)-1-(propionlpiperidin-4-yl)-phenyl)urea

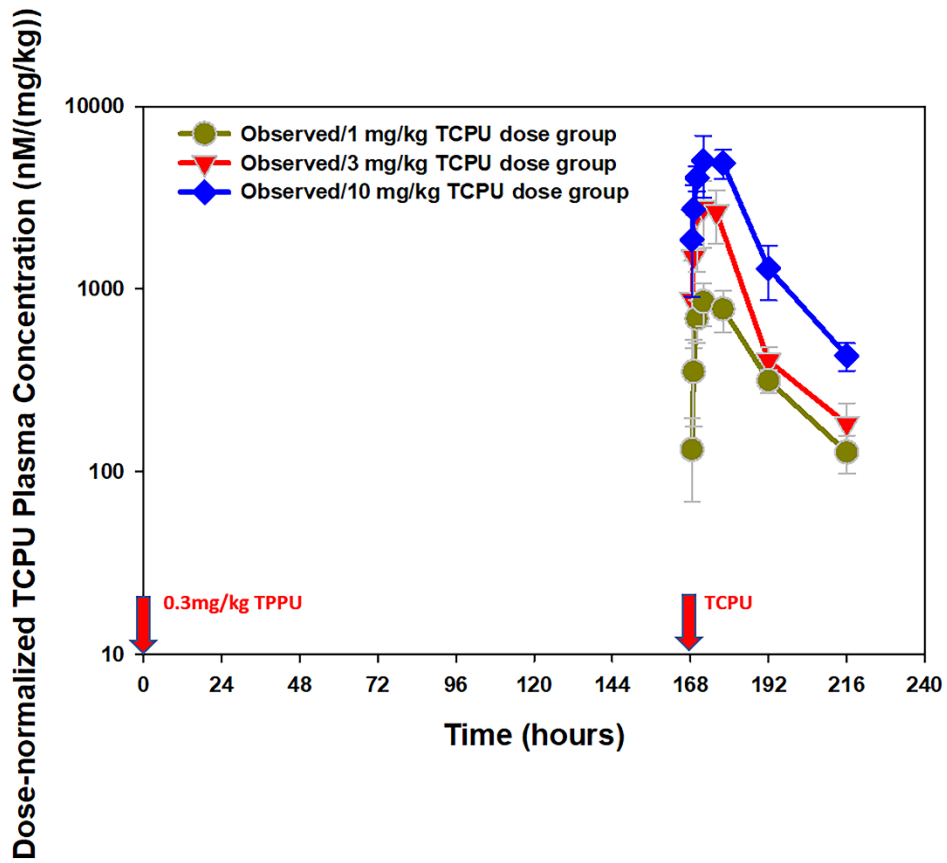
Supplemental Figure 2. Four model structures proposed during model development phase. Model with one TMDD component. b) Model with two TMDD components. c) Model with two TMDD components plus MM process. d) Model with two TMDD components mixing with competitive and non-competitive mechanism.



Supplemental Figure 3. Time courses of mean observed TPPU plasma concentrations following 0.3 mg/kg TPPU at time 0 in a) sEH deficient mice without TCPU displacement; b) wild-type mice without TCPU displacement; and c) wild-type mice with 3 mg/kg TCPU displacement at 168 hours.



Supplemental Figure 4. Time courses of mean observed TCPU plasma concentrations following 0.3 mg/kg TPPU at time 0 in wild-type mice with 1,3, 10mg/kg TCPU displacement at 168 hours.



Supplemental Figure 5. Visual Predictive Check (VPC) for a) TPPU in sEH knockout mic; b) TPPU in wild-type mice; and c) TCPU in wild-type mice. The open triangles represent the observed concentrations, the dashed lines represent the 5th, 50th, and 95th percentiles for the observed data, and the solid lines represent the 5th, 50th, and 95th of the prediction percentiles

